JOURNAL OF KUFA–PHYSICS
journal.uokufa.edu.iq/index.php/jkp/index | ISSN: 2077–5830

Effect of the preparation temperature of titanium dioxide deposited on Si wafers on the UV response of the detector

Basheer Kadhim Hassan Al-Mayyahi[1,2], Mohammad Akbarzadeh Pasha[1] and Husam S. Al-Salman[3]

[1]Faculty of Science, University of Mazandaran, Mazandaran, Iran.
[2]Directorate of Education in Al Basrah, Ministry of Education, Basrah, Iraq.
[3]Faculty of Science, University of Basrah, Basrah, Iraq

*Corresponding Author E-mail: Basheerkadhim38@gmail.com, makbarzadehpasha@gmail.com, husam.jasim@uobasrah.edu.iq

ARTICLE INF.

Article history:
Received: 12 SEP., 2025
Revised: 13 DEC., 2025
Accepted: 24 DEC., 2025
Available Online: 29 DEC. 2025

Keywords:

Anatase and rutile phases
annealing effect TiO_2 nanorods
hydrothermal method
surface morphology

ABSTRACT

In this study, nanocomposite films of titanium oxide (TiO_2) were prepared on Si plates by hydrothermal method at high temperatures (i.e.150 °C, 160 °C and 170 °C) with the concentration of titanium oxide was fixed at 0.75 ml and the deposition time constant at 6 h. These films were prepared by adding 0.75 ml of titanium butoxide (TiO_2), 20 ml of hydrochloric acid and 40 ml of deionized water. The heat treatment was carried out at 450 °C for 2 hrs. UV-vis tests were performed on FTO samples (T1, T2 and T3) at different temperatures, when the absorbance and energy gaps of the samples were studied. XRD examinations showed the peaks of each sample, and FESEM images also showed the shapes of nanorods for all samples. With using a photoluminescence device, it was found that the photoluminescence value was concentrated at (415 - 405 nm) in the samples prepared with TiO_2, and its intensity was observed to increase with increasing temperature. Si/TiO2 photodetectors prepared at different temperatures. The sensitivity (844%, 500% and 440%) and photoresponse (0.0152, 0.0075 and 0.00585 A/W) were obtained for the temperatures (150 °C, 160 °C and 170 °C), respectively. These parameters were calculated using UV light with a wavelength of 385 nm and an intensity of 0.05 mW/cm^2 at a room temperature, applying a bias voltage of 3 V, consistent with the electrical configuration used during photoresponse measurements with an on time of 20 s and off time of 20 s. These rays were incident perpendicularly on the photodetectors at a distance of 5 cm. In this study, we will focus on the best results obtained from the measurements.

DOI: https://doi.org/10.31257/2018/JKP/2025/v17.i02.21439

تأثير درجة حرارة تحضير ثاني أكسيد التيتانيوم المترسب على رقائق السيليكون على استجابة الأشعة فوق البنفسجية للكاشف

بشير كاظم حسن المياحي[1،2]، محمد أكبرزاده باشا[1]
وحسام السلمان[3]

[١]كلية العلوم، جامعة مازندران، مازندران، إيران.
[٢]مديرية التربية والتعليم في البصرة، وزارة التربية والتعليم، البصرة، العراق.
[٣]كلية العلوم، جامعة البصرة، البصرة، العراق

الـــخُـــلاصـــة

في هذه الدراسة، تم تحضير أغشية نانوية مركبة من أكسيد التيتانيوم (TiO_2) على ألواح سيليكون باستخدام الطريقة الحرارية المائية عند درجات حرارة عالية (150 درجة مئوية، 160 درجة مئوية، و170 درجة مئوية)، مع تركيز أكسيد التيتانيوم ثابت عند 0.75 مل، وثابت زمن الترسيب 6 ساعات. حُضِّرت هذه الأغشية بإضافة 0.75 مل من بوتوكسيد التيتانيوم(TiO_2) ، و20 مل من حمض الهيدروكلوريك، و40 مل من الماء منزوع الأيونات. أُجريت المعالجة الحرارية عند درجة حرارة 450 درجة مئوية لمدة ساعتين. أُجريت اختبارات الأشعة فوق البنفسجية والمرئية على عينات بوتوكسيد التيتانيوم(T1) ، T2، و (T3عند درجات حرارة مختلفة، ودُرِسَت فجوات الامتصاص والطاقة في العينات. أظهرت فحوصات حيود الأشعة السينية (XRD) قمم كل عينة، كما أظهرت صور المجهر الإلكتروني أشكال القضبان النانوية لجميع العينات. باستخدام جهاز التلألؤ الضوئي، وجد أن قيمة التلألؤ الضوئي كانت مركزة عند (415 - 405 نانومتر) في العينات المحضرة باستخدام TiO2، ولوحظ أن شدتها تزداد مع زيادة درجة الحرارة. أجهزة الكشف الضوئي Si/TiO_2 المحضرة عند درجات حرارة مختلفة تم الحصول على الحساسية (844٪، 500٪ و440٪) والاستجابة الضوئية (0.0152، 0.0075 و0.00585 A/W) لدرجات الحرارة (150 درجة مئوية، 160 درجة مئوية و170 درجة مئوية) على التوالي. تم حساب هذه المعلمات باستخدام ضوء الأشعة فوق البنفسجية بطول موجي 385 نانومتر وكثافة 0.05 مللي واط / سم 2 في درجة حرارة الغرفة، وتطبيق جهد تحيز (0 فولت) مع طاقة ذاتية، وزمن تشغيل 20 ثانية وزمن إيقاف 20 ثانية. سقطت هذه الأشعة عموديًا على أجهزة الكشف الضوئي على مسافة 5 سم. وفي هذه الدراسة سوف نركز على أفضل النتائج التي تم الحصول عليها من القياسات.

الكلمات المفتاحية:

طور الأناتاز والروتيل

قضبان نانوية من ثاني أكسيد التيتانيوم ذات تأثير التلدين الطريقة الحرارية المائية مورفولوجيا السطح.

1. INTRODUCTION

Titania (TiO_2) is one of the well-known titanium compounds that is often used in various applications. These applications include self-cleaning coatings, anti-corrosion coatings, photo-voltaics, photocatalysis, photodetectors, and dye-composite solar [1, 2]. There are three different phases of the crystal form of TiO_2: rutile, anatase (tetragonal structure), and brookite (orthorhombic structure) phases [3, 4]. Both rutile and anatase belong to different phase groups although they have a tetragonal crystal structure. Rutile TiO_2 has higher (electrical resistivity, refractive index, chemical stability and dielectric constant) than those of the anatase phase [5]. Titanium dioxide is known to be a very useful, non-toxic, environmentally friendly, sunscreen and corrosion-resistant substance, and it is often used in white paint and pigments due to its white color. It is an n-type semiconducting material with an

energy bandgap of 3.02 eV for rutile, 3.23 eV for anatase, and 3.13 eV for brookite [6-8]. TiO_2 can be grown using many different methods.

This includes spraying, chloride process spray pyrolysis, chemical vapor deposition and Sol-gel method [8], physical vapor deposition (PVD) and the hydrothermal method [7, 9]. Hydrothermal synthesis is the method that is used to manufacture materials at low temperatures with high vapor pressure. Since the reaction occurs in closed system conditions, this method is considered the most environmentally, friendly and energy-saving [10]. Teflon-lined stainless steel autoclave is usually used for hydrothermal synthesis under controllable temperature in aqueous solutions [11]. Materials manufactured by the hydrothermal method have many qualities. These include high purity, good homogeneity and crystalline integrity with fine grain size distribution [12]. The hydrothermal method is a successful way to prepare titanium oxide, zinc oxide and other remarkable materials [13]. Recent studies have further demonstrated the importance of optimized hydrothermal conditions for improving TiO_2 nanorod crystallinity and enhancing UV photodetection performance [14-16].

In this work, TiO_2 nanofilms were synthesized using an uncomplicated hydrothermal method at reaction temperature (150 °C, 160 °C and170 °C) and time of (6 h). The effect of high annealing temperatures (450 °C) on the structural composition, surface morphology and optical band gap was studied.

2. Experimental details

2.1 Materials and methods

Hydrochloric acid (HCl) (SDFCL, 35.4%) was used. Si plates were used as a substrate to deposit a thin layer of TiO_2. Distilled and deionized water was used. 20 mL of HCl was mixed with 40 mL of distilled and deionized water using a magnetic stirrer for 20 min. 0.75 mL of titanium butoxidewas added to the mixture and a magnetic stirrer for 20 min was used as well. The titanium precursor used in this study was titanium (IV) butoxide ($Ti(OBu)_4$, ≥ 97% purity, Sigma-Aldrich). In the acidic medium of HCl, titanium butoxide undergoes controlled hydrolysis and proton-assisted decomposition, forming Ti^{4+} species that serve as nucleation centers for TiO_2 nanorod growth during the hydrothermal process.

Then two Si plates were vertically inserted into the Teflon-lined layer, which were previously cleaned by ultrasonication in the sequence of propanol and acetone for 15 mins. 40 mL of the prepared solution was added to a Teflon-lined stainless steel pressure vessel (100 mL), and heated in an oven at different temperatures (150 °C, 160 °C, 170 °C) for 6 h. Then it was left to self-cool to a room temperature, then the materials were taken out of the autoclave, dried and heat treated at 450°C for 2 hrs. Finally, a white layer of titanium dioxide was obtained on the surface of the Si material.

2.1.1 Sample Naming and Experimental Variables

In this study, three TiO_2/Si samples were prepared under identical precursor composition and reaction time, while

varying only the hydrothermal temperature. To simplify discussion throughout the manuscript, each sample is assigned a specific label based on its growth temperature. Table 1 summarizes the naming scheme and the corresponding synthesis variable.

Table 1. Sample codes and corresponding hydrothermal temperatures.

Sample Cod	Hydrothermal Temperature (°C)	Constant Parameters
T1	150	Ti precursor = 0.75 mL, HCl = 20 mL, DI water = 40 mL, reaction time = 6 h
T2	160	
T3	170	

2.2 Characterizations

Structural characterizations of TiO_2 nanostructure films were performed using X-ray diffraction (X-Ray Diffractometer, DX-2700) with Cu kα. The scanning angle varied in the range of (10-70) ° at a room temperature with a wavelength of 1.5406 Å. The surface morphologies were characterized using field mission scanning electron microscope FE-SEM (FEI FESEM Nova 450, FEI-Netherlands- Holland). The optical characterization was studied from the outcome of the absorbance and transmittance in the UV-Vis region (300-900) nm using a double beam Mega 2100-Sinco UV-Vis spectrophotometer.

3. Results and discussion

Regarding the XRD of samples T5, T6, and T7 of titanium dioxide with silicon, Figure (1) represents samples P-Si/TiO_2 (at 150 °C, 160 °C and 170 °C) for 6 hrs. The results showed many different peaks for TiO_2 and Si, at 2θ = 27.9 , 36.4 , 41.5 , 44.7 , 54.1 and 57,7 belong to the (110) , (101) , (111) , (210) , (211) and (220) surfaces respectively for TiO_2 . Concerning the result of Si, it was found that the highest peak at 2θ = 69.36 which corresponds to (311) .The first Figures 1A, 1B represent the XRD for (n-TiO_2/p-Si) at different temperature and the second Figure after zoom to show all peaks. These findings are in agreement with the JCPDS-72-1426 card.

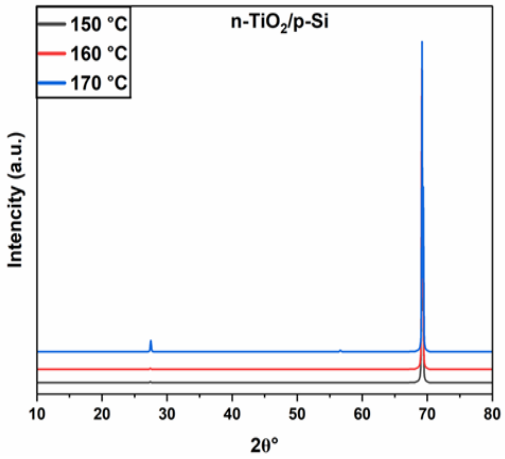

Fig. 1A. XRD pattern of TiO_2/Si samples (T1–T3) at different hydrothermal temperatures.

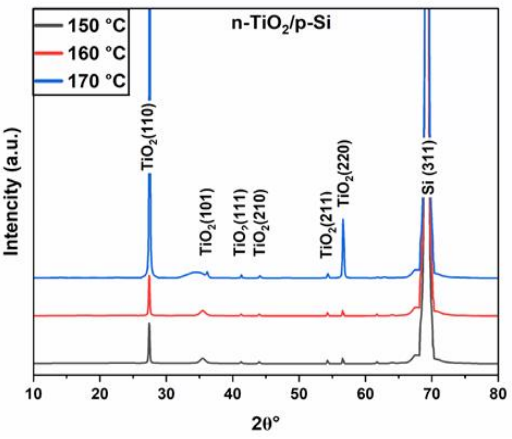

Fig. 1B. Magnified XRD pattern showing detailed peak structure for the TiO_2/Si samples.

As for silicon, it must be treated by scratching, or what is called etching, using hydrofluoric acid (HF) and silver nitrate ($AgNo_3$) in order to increase the adhesion of the film to the silicon and its stability on the surface, as hydrofluoric acid and silver nitrate represent only auxiliary factors and have nothing to do with the composition of the TiO_2 layer.

The film image shows TiO_2 and it looks like a nanorod with a diameter of approx (370 - 634) nm. And, the cross-section of TiO_2 film which has a length of about (807) nm. Fig. (2) shows the Scanning electron microscope images of TiO_2 films on Si bases (T1).

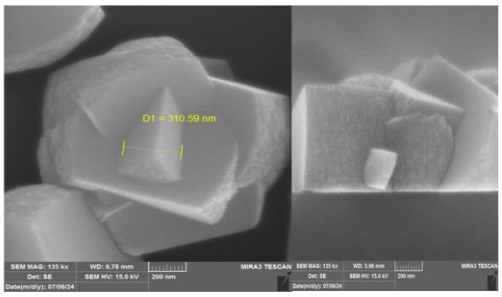

Fig. 2. FESEM images of sample T1 (150 °C) at different magnifications.

Fig. (2) Scanning electron microscope images of TiO_2 films prepared by the hydrothermal method on Si b*a*ses at a temperature of 150°C and a deposition time of 6 h (T1 Sample) The film image shows TiO_2 and it looks like a nanorod with a diameter of approx (370 - 634) nm. And the cross-section of TiO_2 film has a length of about (807) nm.

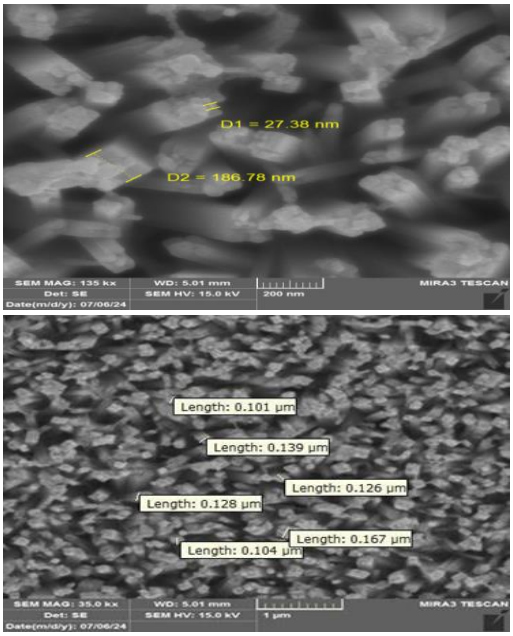

Fig. 3. FESEM images of sample T2 (160 °C) at different magnifications.

Fig. (3) Scanning electron microscope images of TiO_2 films prepared by the hydrothermal method on Si bases at a temperature of 160 °C and a deposition time of 6 h (T2 Sample) The film image shows TiO_2 and it looks like a nanorod with a diameter of approx. (101 - 167).

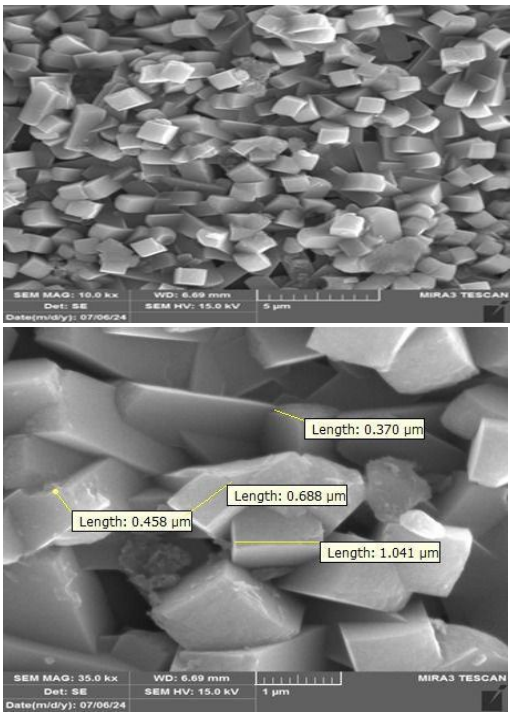

Fig. 4. FESEM images of sample T3 (170 °C) at different magnifications.

Fig. (4) Scanning electron microscope images of TiO_2 films prepared by the hydrothermal method on Si b*a*ses at a temperature of 170 °C and a deposition time of 6 h (T3 Sample) Image of the surface at magnification of 5 µm. The film image shows TiO_2 and it looks like a nanorod with a diameter of approx. (370 - 1041) nm. And the cross-section of TiO_2 film, which has a length about (2050) nm. An increase in the hydrothermal temperature significantly affects the nucleation and growth kinetics of TiO_2 nanorods. Higher temperatures enhance crystal rearrangement and oxygen vacancy formation, which directly impacts the optical bandgap, PL emission intensity, and charge carrier mobility. These structural modifications explain the observed enhancement in carrier generation under UV illumination and the variation in response and recovery times. Therefore, the differences in photodetector performance among samples T1, T2, and T3 are strongly correlated with temperature-dependent crystal quality and defect density.

Photoluminescence (PL) or instantaneous luminescence is a phenomenon in which a particular substance emits light after it absorbs light or electromagnetic energy. When a substance is exposed to light, the electrons in the atoms and molecules of the substance move to a higher energy level. When these electrons return to lower energy levels, the energy is released in the form of photons, causing Fluorescence spectrum. Photoluminescence spectrum of TiO_2 films at room temperature prepared on silicon bases using the hydrothermal method at different temperatures (150 °C, 160 °C and 170 °C). The photoluminescence spectra were obtained using an excitation wavelength of 330 nm, corresponding to the near-UV photon energy suitable for generating electron–hole pairs in TiO_2.

Using an excitation wavelength of 330 nm, the spectra show an emission peak at as shown in the figure (3.20) that is, upon excitation using band gap energy, the photoexcited electrons fall to the lowest level in the excited state [17]. When TiO_2 is exposed to light, it reconstructs a hole with the electron and emits light photons [18]. This description of electron–hole recombination and photon emission is consistent with standard PL mechanisms reported in TiO_2 nanostructures .[19]

The plot is titled (T1) Si at 150 ^{o}C. The emission peak appeared at about 450 nm in the intensity 180 (count sec $^{-1}$). The bandgap energy was calculated using the standard photon energy relation (Equation 1), which is widely applied for optical transitions in semiconductors[20].

$$Eg = \frac{1240}{\lambda} \qquad (1)$$

The band gap is 2.75 eV

The plot is titled (T2) Si at 160 ^{o}C. The emission peak appeared about 445 nm in the intensity 110 (count sec $^{-1}$).

The energy gap can be calculated using the equation (1). The band gap is 2.78 eV

The plot is titled (T3) Si at 170 ºC. The emission peak appeared at about 450 nm in the intensity 190 (count sec $^{-1}$). The energy gap can be calculated using the equation (1). The band gap is 2.75 ev.

Figure (5) shows that as the temperature increases, the peaks shift toward shorter wavelengths with a decrease in intensity

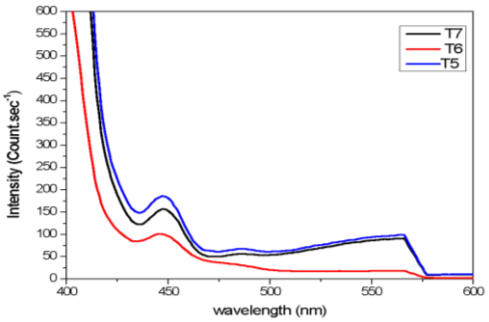

Fig. 5. Photoluminescence spectra of TiO_2/Si samples at different synthesis temperatures.

Current – Voltage Characteristics

Among the electrical characteristics through which the performance of the TiO_2/Si photodetector is described are the (current - voltage) characteristics, which explain the behavior of the current with the voltages applied to the detector. The electrical properties of photodetectors were studied in the dark and in the presence of light, using a Keithley 2400 device. Figure (6) shows the change in the amount of electrical current with changing temperature, on time of 20 seconds, and off time of 20 seconds, using ultraviolet radiation with a wavelength of 385 nm and an intensity of 0.05 mW/cm^2 at a room temperature. All measurements shown in Figure 6 were performed under an applied bias of 3 V, which was used for all subsequent photoresponse and sensitivity calculations. These rays were directed vertically at the sample at a distance of (5 cm), where a decrease in electric current value was observed with change in temperature.

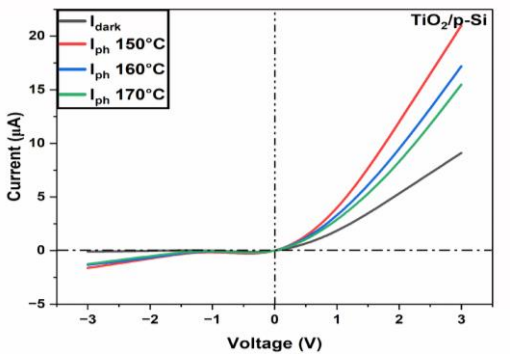

Fig. 6. Current–voltage characteristics of TiO_2/Si photodetectors under UV illumination.

Photoresponse measurements of TiO_2/Si photodetectors prepared by the hydrothermal method were performed at different temperatures, using UV light with a wavelength of 385 nm and an intensity of 0.05 mw/cm^2 at room temperature, a bias voltage of zero volt , and an (operation, extinguishing)time of 20 seconds. AThese rays were directed vertically at the photodetectors at a distance of 5cm, and the optical response and sensitivity were calculated using equations [21, 22]:

$$R_\lambda = \frac{I_{ph}}{P_{in}} \qquad (2)$$

$$S = \frac{I_{ph} - I_{dark}}{I_d} * 100\% \qquad (3)$$

It has been found that the work of photodiodes is to generate electron gap pairs by absorbing incident light. The rise time was then calculated, which means the response time of the photodetector with a time difference between 10% and 90% of the maximum optical current.

The efficiency values listed in Table 2 were calculated using the external quantum efficiency (EQE%) expression [23]:

$$EQE\% = \frac{R \times hc}{e\lambda} \times 100 \qquad (4)$$

where R is the responsivity (A/W), h is Planck's constant, c is the speed of light, e is the elementary charge, and λ is the wavelength of the incident UV light (385 nm in this study). This method is widely used for evaluating the performance of TiO_2-based UV photodetectors. The obtained EQE values reflect the efficiency of converting incident photons into measurable photocurrent.

In addition to calculating the fall time, the results at figure (7) were as follows:

Table 2. The results of photodetectors at different temperatures for TiO_2/Si

sample	Temp	T_{rise}(s)	T_{fall}(s)	Idark	Iph	Sph %	R(A/W)	η %
T5	150 °C	3.13	1.71	0.018	0.17	844	0.0152	4.9
T6	160 °C	4.12	1.94	0.015	0.09	500	0.0075	2.4
T7	170 °C	5.08	3.29	0.0133	0.0718	440	0.00585	1.9

The first model, T1 (TiO_2/Si), prepared at a temperature of 150oC, had a rise time of 3.13 s, a fall time of 1.71 s, a dark current of 0.018 µA, a photocurrent of 0.17 µA, a sensitivity of 844%, a photoresponse of 0.0152 A/W, and an efficiency of 24.9%.

The second model, T2 (TiO_2/Si), prepared at a temperature of 160oC, had a rise time of 4/12 s, a fall time of 1.94 s, a dark current of 0.015 µA, a photocurrent of 0.09 µA, a sensitivity of 500%, a photoresponse of 0.0075 A/W, and an efficiency of 2.4 %

The third model, T3 (TiO_2/Si), prepared at a temperature of 170 °C, had a rise

time of 5.08 s, a fall time of 3.29 s, a dark current of 0.0133 µA, a photocurrent of 0.0718 µA, a sensitivity of 440%, a photoresponse of 0.00585 A/W, and an efficiency of 1.9 %.

Fig. (7) Show the Time response of the detector T1, T2 and T3 at different temperatures (150 °C, 160 °C, and 170 °C) for (TiO_2/Si). All time-response measurements shown in Figure 7 were recorded under an applied bias of 3 V, identical to the configuration used for the photocurrent measurements in Figure 6.

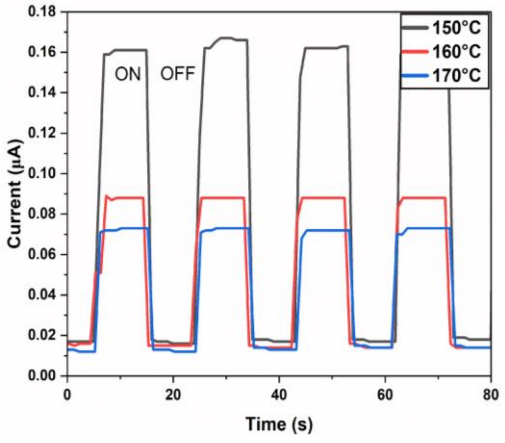

Fig. 7. Time-response curves (rise and fall times) of TiO_2/Si photodetectors

(T1, T2, T3) measured under 385 nm UV illumination at an applied bias of 3 V.

To clarify the extraction of the temporal response parameters, a schematic illustration is provided in Fig. (8). The rise time (τ_{rise}) is defined as the time interval required for the photocurrent to increase from 10% to 90% of its maximum steady-state value (I_{max}) upon UV illumination, while the fall time (τ_{fall}) corresponds to the time required for the photocurrent to decay from 90% to 10% of I_{max} after switching off the UV source. This method was used to extract the response times reported in Table 2.

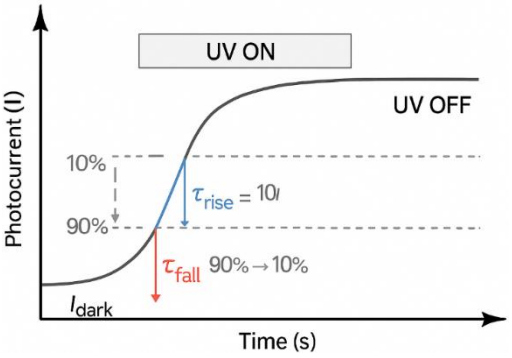

Fig. 8. Schematic illustration of the extraction of rise time (τ_{rise}, 10–90%) and fall time (τ_{fall}, 90–10%) from the time-response curve of TiO_2/Si photodetectors under UV illumination, where I_{max} represents the steady-state photocurrent and Idark denotes the dark current.

4- Conclusion

TiO_2 nanorods were successfully synthesized on Si substrate by hydrothermal method. The deposition parameters and conditions were as follows: Hydrochloric acid (HCl) (SDFCL, 35.4%) was used. Si plates were used as the substrate for deposition of TiO_2 thin films. Distilled and deionized water was used. 40 mL of HCl was mixed with 20 mL of distilled and deionized water using a magnetic stirrer for 20 min. Add 0.5 mL of TiO_2 to the mixture and use a magnetic stirrer for 20 min as well.

TiO_2 nanorods were arranged in the xz plane, i.e. they prefer to grow in the plane (101) of the tetragonal anatase TiO_2 crystal. XRD results show the successfully fabricated TiO_2 nanorods with the desired size and preferential anatase phase using titanum botoxide as a starting material. The obtained results indicate that TiO_2 material is very suitable for photovoltaics and photocatalysis applications.

ACKNOWLEDGEMENTS

The authors are very grateful for the assistance provided by the Department of Physics, College of Science, University of Basra, Iraq, Professor Dr. Sattar Jabbar Qasim, Department of Physics, College of Science, University of Basra, Assistant Professor Dr. Alaa Abdel Halim, College of Science, University of Basra, and Dr. Ghaith Abdel Razzaq, College of Science, University of Basra, and Dr.Ameer Farhan, College of Science, University of Kufa.

5 - References

[1] V. Caratto, B. Aliakbarian, A. Casazza, L. Setti, C. Bernini, P. Perego, *et al.*, "Inactivation of Escherichia coli on anatase and rutile nanoparticles using UV and fluorescent light," *Materials Research Bulletin,* vol. 48, pp. 2095-2101, 2013.

[2] H. Khojasteh, B. Khezri, K. Heydaryan, N. Sharifi, P. Aspoukeh, S. Khanahmadzadeh, *et al.*, "Enhancing visible light-driven photocatalysis for water treatment: optimizing Fe3O4@ SiO_2@Cr–TiO_2–S nanocomposite

efficiency with silver and palladium deposition," *Plasmonics,* vol. 20, pp. 817-834, 2025.

[3] C.-J. Li, G.-R. Xu, B. Zhang, and J. R. Gong, "High selectivity in visible-light-driven partial photocatalytic oxidation of benzyl alcohol into benzaldehyde over single-crystalline rutile TiO_2 nanorods," *Applied Catalysis B: Environmental,* vol. 115, pp. 201-208, 2012.

[4] L. M. Anaya-Esparza, Z. Villagrán-de la Mora, J. M. Ruvalcaba-Gómez, R. Romero-Toledo, T. Sandoval-Contreras, S. Aguilera-Aguirre*, et al.*, "Use of titanium dioxide (TiO_2) nanoparticles as reinforcement agent of polysaccharide-based materials," *Processes,* vol. 8, p. 1395, 2020.

[5] J. Jeon, M. Jang, G. M. Park, M. Kim, J. Kim, S. Ye*, et al.*, "Strain-Driven Selective Stabilization of Metastable TiO_2 Phases," *Small,* p. e05427, 2025.

[6] A. MortezaAli and S. R. Sani, "Study of growth parameters on structural properties of TiO_2 nanowires," *Journal of Nanostructure in Chemistry,* vol. 3, p. 35, 2013.

[7] R. Chandoliya, S. Sharma, V. Sharma, R. Joshi, and I. Sivanesan, "Titanium dioxide nanoparticle: A comprehensive review on synthesis, applications and toxicity," *Plants,* vol. 13, p. 2964, 2024.

[8] S. A. H. Moradi, D. A. Oleiwi, K. Heydaryan, S. H. Abed, and F. Namvar, "UV-Responsive Er-Doped $NiAl_2O_4$/Mn/GO Nanocomposites: Green Synthesis and Photocatalytic Degradation of Organic Pollutants via Fluorescent Behavior for Water Purification," *Journal of Fluorescence,* pp. 1-19, 2025.

[9] C. A. Beaudette, Q. Tu, M. Ali Eslamisaray, and U. R. Kortshagen, "Plasma-Synthesized Nitrogen-Doped Titanium Dioxide Nanoparticles With Tunable Visible Light Absorption and Photocatalytic Activity," *ASME Open Journal of Engineering,* vol. 1, 2022.

[10] X. Ren, K. Senapati, W.-T. Jiang, and C.-H. Jiang, "Formation of ordered TiO2 nanostructural arrays with tunable shapes by magnetron sputtering method," *Materials Chemistry and Physics,* vol. 126, pp. 1-5, 2011.

[11] A. M. Selman and Z. Hassan, "Influence of deposition temperature on the growth of rutile TiO_2 nanostructures by CBD method on seed layer prepared by RF magnetron sputtering," *Superlattices and Microstructures,* vol. 64, pp. 27-36, 2013.

[12] Z. Luo, W. Yang, A. Peng, Y. Zeng, and J. Yao, "The fabrication of TiO2 nanorods from TiO_2 nanoparticles by organic protection assisted template method," *Nanotechnology,* vol. 20, p. 345601, 2009.

[13] S. K. Pradhan, P. J. Reucroft, F. Yang, and A. Dozier, "Growth of TiO_2 nanorods by metalorganic chemical vapor deposition," *Journal of Crystal Growth,* vol. 256, pp. 83-88, 2003.

[14] O. Adedokun, A. O. Muraina, P. R. Jubu, O. S. Obaseki, O. M. Adedokun, M. D. Ooi*, et al.*, "Reaction duration impact on morphological, optical, structural and photoelectrochemical properties of hydrothermally synthesized TiO_2 nanorods," *Zeitschrift für Physikalische Chemie,* vol. 239, pp. 1169-1184, 2025.

[15] L. Wu, X. Shi, H. Fan, Q. Li, P. Hu, and F. Teng, "Self-Powered Broadband Photodetector Based on Pyramid-Structured-Si/TiO_2 Heterojunction," *Chinese Physics B,* 2025.

[16] N. Shakeel, I. Piwoński, A. Kisielewska, M. Krzywiecki, D. Batory, and M. Cichomski, "Morphology-Dependent Photocatalytic Activity of Nanostructured Titanium Dioxide Coatings with Silver Nanoparticles," *International Journal of Molecular Sciences,* vol. 25, p. 8824, 2024.

[17] M. Rajabi and S. Shogh, "Defect study of TiO_2 nanorods grown by a hydrothermal method through photoluminescence spectroscopy," *Journal of Luminescence,* vol. 157, pp. 235-242, 2015.

[18] M. Vishwas, K. N. Rao, and R. Chakradhar, "Influence of annealing temperature on Raman and photoluminescence spectra of electron beam evaporated TiO_2 thin films," *Spectrochimica Acta Part A: Molecular and Biomolecular Spectroscopy,* vol. 99, pp. 33-36, 2012.

[19] D. K. Pallotti, L. Passoni, P. Maddalena, F. Di Fonzo, and S. Lettieri, "Photoluminescence mechanisms in anatase and rutile TiO_2," *The Journal of Physical Chemistry C,* vol. 121, pp. 9011-9021, 2017.

[20] S. Sahare, M. M. Solovan, A. I. Mostovyi, H. P. Parkhomenko, N. Schopp, M. Ziółek*, et al.*, "Semiconductor Bandgap Measurements: Overview of Optical, Electrical, and Device-Level Techniques," *Advanced Optical Materials,* vol. 13, p. e01747, 2025.

[21] A. M. Arjmandi-Tash, A. Mansourian, F. R. Rahsepar, and Y. Abdi, "Predicting photodetector responsivity through machine learning," *Advanced Theory and Simulations,* vol. 7, p. 2301219, 2024.

[22] H. Hashemnezhad and M. Noori, "Zero-biased graphene photodetector with high responsivity integrated into silicon microring resonator," *Scientific Reports,* vol. 15, p. 27701, 2025.

[23] H. Ma, H. Fang, Y. Liu, J. Li, K. Jing, J. Hong*, et al.*, "Fully transparent ultraviolet photodetector with ultrahigh responsivity enhanced by MXene-induced photogating effect," *Advanced Optical Materials,* vol. 11, p. 2300393, 2023.